THE TIME-REVERSAL TECHNIQUE RE-INTERPRETED: SUBSPACE-BASED SIGNAL PROCESSING FOR MULTI-STATIC TARGET LOCATION *

Hanoch Lev-Ari and Anthony J. Devaney

Department of Electrical and Computer Engineering
Northeastern University, Boston, MA 02115

ABSTRACT

The *time-reversal field processing* technique for active remote sensing is re-interpreted in the conceptual framework of subspace-based signal processing. Although both of these subjects have a long and extensive history, we believe that our work is the first to relate these two rather different signal processing approaches. The concept at the heart of both approaches is the multi-static *Frequency Response Matrix* (FRM) of the active antenna array. It is a function of array/scatterer geometry (via a suitable Green function) and of the scatterers' reflection coefficients. The time-reversal technique locates the most reflective target by determining the largest singular value of the FRM and the corresponding (right) singular vector. Consequently, it performs well only when the scatterers are "well-resolved," i.e., when the Green function vectors used in forming the FRM are approximately orthogonal to each other. In contrast, we show that subspace-based signal processing can be successfully used even when the targets are not "well-resolved." Moreover, the performance of our subspace-based schemes can be further enhanced by using wideband signals and combining FRM information from multiple frequencies. The coupling of time-reversal field processing with subspace methods leads to a powerful approach for locating targets under arbitrary wave-propagation conditions (both near-field and far-field), including arbitrary non-homogeneous media and arbitrary geometries.

1. INTRODUCTION

Two methodologies that have received considerable attention in the general area of array processing are *time-reversal imaging* [1, 2, 3, 4] and subspace-based processing [5, 6]. In time-reversal imaging one or more unknown targets (scatterers) are sequentially probed using a set of N antennas, and the backscattered returns are measured at all the antenna locations yielding the so-called *Frequency Response Matrix* $\mathcal{H}(\omega) = \{H_{ij}(\omega);\ 1 \leq i,j \leq N\}$, where $H_{ij}(\omega)$ denotes the response (at frequency ω) between the i-th element and the j-th element of the array. This (multi-static) frequency response matrix is then used to compute the Hermitian *time-reversal matrix* $\mathcal{H}^H(\omega)\mathcal{H}(\omega)$ whose eigenvectors can be shown to correspond, in a one-to-one manner, with the different targets[1]. In particular, the wavefield generated from the array when excited by one of these eigenvectors focuses on the associated target, so that if the Green function of the background medium in which the targets are embedded is known, a synthetic image of the target locations is easily computed [1, 2, 4].

In this paper we describe how subspace-based methods can also be used in conjunction with active antenna array systems and, in particular, can be applied to the problem of locating L point targets $(L < N)$ from the measured $N \times N$ multi-static response matrix $\mathcal{H}(\omega)$ of the antenna array. In place of the array covariance matrix, which forms the basis for the classical MUSIC and related techniques [5], the scheme described here employs the $N \times N$ FRM $\mathcal{H}(\omega)$, whose singular vectors play the same role as the eigenvectors of the MUSIC covariance matrix. Thus, the coupling of time-reversal field processing with subspace-based methods, leads to a powerful approach for detecting and locating targets in both homogeneous and non-homogeneous backgrounds, especially in cases of closely spaced targets and/or very sparse antenna arrays, as are employed, for example, in the *TechSat 21* program under consideration by the Air Force.

The key property of multi-static antenna arrays that makes them suitable for applying subspace-based signal processing schemes is the rank-deficiency of the fre-

*This work was supported in part by the Air Force under contracts F41624-99-D6002 and F49620-99-C-0013.

[1]This statement is true only if the targets are well-resolved.

quency response matrix: the rank of the FRM equals (in the absence of noise) to the number of individual point scatterers present. We exploit this property to construct a target location and identification algorithm based on the concept of signal and noise subspaces, as described in Sec. 3.

The paper is directed primarily at *near field* target detection and location estimation where the target separation is sufficient, where multiple scattering between different targets can be ignored and the Born approximation used. Also, the theory is developed entirely in the frequency domain, and so applies equally to narrow-band or broad-band antenna elements. Finally, it should be mentioned that although the theory is developed for point scatterers and ideal point (monopole) antenna elements, the generalization to continuously distributed targets and realistic antennas is not difficult, and is currently under development.

2. MATHEMATICAL FORMULATION

We consider a (generally 3D) array of N antennas, centered at the space points $\mathbf{R}_j$, for $j = 1, 2, \ldots, N$. Each antenna radiates energy into a half space in which are embedded L scatterers, centered at the space points $\mathbf{X}_k$, for $k = 1, 2, \ldots, L$. By exciting a single element of the array with a suitable signal we can measure the frequency response between this element and all the other elements of the array. These measurements determine the array's frequency response matrix $\mathcal{H}(\omega) = \left[H_{ij}(\omega)\right]_{i,j=1}^{N}$ Due to reciprocity, $H_{ij}(\omega) = H_{ji}(\omega)$, so that $\mathcal{H}(\omega)$ is a symmetric matrix, namely $\mathcal{H}^T(\omega) = \mathcal{H}(\omega)$ for each ω.

The frequency response matrix (FRM) is a function of the geometry and physics of wave propagation between the antenna elements and the scatterers, as expressed by the associated Green function $G(\mathbf{R}_i, \mathbf{X}_k; \omega)$. This function includes the effects of: (i) array geometry, (ii) scatterers' geometry, (iii) medium characteristics, including non-homogeneities, and (iv) directivity patterns of the antenna elements and the scatterers. The FRM also depends on the frequency-dependent scattering properties of each target, which can be expressed in terms of the reflection coefficients $\rho_k(\omega)$. Thus,

$$H_{ij}(\omega) = \sum_{k=1}^{L} G(\mathbf{R}_i, \mathbf{X}_k; \omega)\, \rho_k(\omega)\, G(\mathbf{X}_k, \mathbf{R}_j; \omega)$$

The reciprocity constraint $H_{ij}(\omega) = H_{ji}(\omega)$ is now automatically enforced by using the same Green function in the transmission (antenna-to-scatterer) path and in the reception (scatterer-to-antenna) path. The resulting expression for the complete FRM is

$$\mathcal{H}(\omega) = \mathcal{G}(\omega)\, \mathcal{R}(\omega)\, \mathcal{G}^T(\omega) \qquad (1a)$$

where $\mathcal{G}(\omega)$ is an $N \times L$ matrix, viz.,

$$\mathcal{G}(\omega) = \left[\Gamma(\mathbf{X}_1; \omega)\ \ \Gamma(\mathbf{X}_2; \omega)\ \ \ldots\ \ \Gamma(\mathbf{X}_L; \omega)\right] \qquad (1b)$$

$$\mathcal{R}(\omega) = \mathrm{diag}\left\{\rho_1(\omega), \rho_2(\omega), \ldots \rho_L(\omega)\right\} \qquad (1c)$$

and $\Gamma(\mathbf{X}_k; \omega)$ is the *steering vector* associated with the k-th scatterer, viz.,

$$\Gamma(\mathbf{X}; \omega) = \left[G(\mathbf{R}_1, \mathbf{X}; \omega)\ \ \ldots\ \ G(\mathbf{R}_N, \mathbf{X}; \omega)\right]^T \qquad (1d)$$

As long as $L < N$, i.e., the number of antenna elements exceeds the number of scatterers, the $N \times N$ frequency response matrix is rank deficient, viz., rank $\mathcal{H}(\omega) \leq L$. This property of the FRM forms the basis for applying subspace-based signal processing techniques to recover the scatterer locations $\mathbf{X}_k$.

The foregoing discussion relies on the assumption that the Green function $G(\mathbf{R}, \mathbf{X}; \omega)$ can be calculated, when required, for any choice of the space points $\mathbf{R}$ and $\mathbf{X}$. This assumption is satisfied in two important cases: (i) homogeneous dispersive and non-dispersive media, and (ii) parallel layered media. We also assume from now on that the matrix $\mathcal{G}(\omega)$ has full (column) rank, so that rank $\mathcal{H}(\omega) = L$. This assumption is satisfied in all but a few non-generic configurations [7].

3. TIME-REVERSAL PROCESSING

In the DORT formulation of time-reversal imaging [2], one determines the eigenvectors of the so-called time-reversal matrix $\mathcal{H}^H(\omega)\mathcal{H}(\omega)$, where the superscript H denotes conjugate transpose. Since the FRM $\mathcal{H}(\omega)$ is rank deficient, the time-reversal matrix has only L non-zero eigenvalues. The corresponding eigenvectors, say $\{E_k(\omega)\,;\ 1 \leq k \leq L\}$ are backpropagated by forming the product $\Gamma^T(\mathbf{X}; \omega)\, E_k(\omega)$, which describes the wavefield radiated by the array from an applied excitation equal to the k-th eigenvector. It is important to note that in order to use this approach it is necessary to know (i.e., have an analytic or computer model) of the background Green function. Thus, *although computation of the eigenvalues and eigenvectors of the time-reversal matrix requires no knowledge of the background, computation of the image field requires knowledge of the background Green function.*

When the scatterers are well resolved, the columns of the matrix $\mathcal{G}(\omega)$ are approximately orthogonal to each other, so that $E_k^*(\omega) \approx \Gamma(\mathbf{X}_k;\omega)/\|\Gamma(\mathbf{X}_k;\omega)\|$, where $\|\cdot\|$ denotes the Euclidean norm of a vector. Consequently, the radiated wavefields focus at target locations. Each eigenvector serves to locate a single scatterer: the target is located at the maximum value of the magnitude of the wavefield corresponding to each individual eigenvector (Fig. 1).

The above result does not, unfortunately, generalize to the case of poorly-resolved targets. In particular, for this more general case, the signal space eigenvectors are linear combinations of the target steering vectors $\Gamma(\mathbf{X}_k;\omega)$. Thus, an applied excitation equal to one of these eigenvectors generates a linear combination of wavefields, each focused on a different target location and each having a different amplitude. Since the targets are not well-resolved, these image fields interfere with each other, so that the quality of the target location estimates suffers. Because of this, the use of focusing to locate and identify non-resolved targets is limited. However, subspace-based methods (such as MUSIC) can be used in these more general situations, as we discuss below.

4. SUBSPACE-BASED PROCESSING

The rank-deficient character of the frequency response matrix $\mathcal{H}(\omega)$ is revealed, for instance, via the singular value decomposition (SVD), which has the form $\mathcal{H}(\omega) = U(\omega)\,\Sigma(\omega)\,V^H(\omega)$, where $U(\omega)$, $V(\omega)$ are $N \times N$ orthogonal matrices. In fact, because the FRM $\mathcal{H}(\omega)$ is symmetric it follows that $V(\omega) = U^*(\omega)$ (where the superscript $*$ denotes conjugation) so that the SVD becomes

$$\mathcal{H}(\omega) = U(\omega)\,\Sigma(\omega)\,U^T(\omega) \qquad (2)$$

The matrix $\Sigma(\omega)$ is diagonal, and its (non-negative) diagonal elements are known as *singular values*. Since $\mathcal{H}(\omega)$ is rank-deficient, all but the first L of the singular values vanish, i.e., $\sigma_1(\omega) \geq \sigma_2(\omega) \geq \ldots \geq \sigma_L(\omega) > 0$, while $\sigma_i(\omega) = 0$ for $i \geq L+1$.

The first L columns of $U(\omega)$ span the same subspace as the columns of $\mathcal{G}(\omega)$, while the remaining $N-L$ columns span the null subspace of $\mathcal{G}(\omega)$. This property can be exploited to provide an implicit characterization of the scatterer locations. Partitioning $U(\omega)$ in the form $U(\omega) = \left[U_s(\omega) \quad U_o(\omega)\right]$, where $U_s(\cdot)$ has L columns, while $U_o(\cdot)$ has $N-L$ columns, we find that $U_o^H(\omega)\,\mathcal{H}(\omega) = 0$. In view of the full (column) rank property of $\mathcal{G}(\omega)$ it follows also that $U_o^H(\omega)\,\mathcal{G}(\omega) = 0$ or, in other words, that

$$\Gamma^H(\mathbf{X}_k;\omega)\,U_o(\omega) = 0 \quad , \qquad \text{for } k = 1,2,\ldots,L \qquad (3)$$

and for each frequency ω. Consequently, $\|\Gamma^H(\mathbf{X}_k;\omega)\,U_o(\omega)\|^2 = 0$ for $k = 1,2,\ldots,L$, and for each frequency ω. While this relation does not hold exactly in the presence of noise and measurement/estimation errors, we can, nevertheless, determine the scatterer locations by searching for local minima of the (scalar) cost function $\|\Gamma^H(\mathbf{X};\omega)\,U_o(\omega)\|^2$. Alternatively, we can construct a *pseudo-distribution* of the MUSIC type [5], viz.,

$$P_{MUSIC}(\mathbf{X},\omega) = \frac{1}{\|\Gamma^H(\mathbf{X};\omega)\,U_o(\omega)\|^2} \qquad (4)$$

which has sharp peaks at the correct target locations (Fig. 1).

The matrices $U(\omega)$, $\Sigma(\omega)$ can also be determined by an eigen-decomposition of the time-reversal matrix $\mathcal{H}^H(\omega)\,\mathcal{H}(\omega)$. This is, in fact, the technique used in the time-reversal processing method [1]. However, it is generally advisable to process the FRM itself rather than one of its squared versions: benefits accrue from the resulting reduction in matrix condition number.

When the FRM is known over a range of frequencies, say for $\omega \in \Omega$, this pseudo-distribution can be improved by integrating over all available frequencies, i.e.,

$$P_{I-MUSIC}(\mathbf{X}) = \frac{1}{\displaystyle\int_{\omega\in\Omega} \|\Gamma^H(\mathbf{X};\omega)\,U_o(\omega)\|^2\,d\omega} \qquad (5)$$

Since the fundamental relation (3) holds for every individual frequency $\omega \in \Omega$ this improved pseudo-distribution still has sharp peaks at the scatterer locations $\mathbf{X}_k$, but it is less likely than $P_{MUSIC}(\mathbf{X};\omega)$ to have significant spurious peaks.

5. SIMULATIONS

To demonstrate the superior resolution achieved with subspace-based processing we consider an example involving two point scatterers, at a distance of 10.0125λ from the array (where λ denotes the wavelength), and separated from each other by 2.025λ. The array is linear, consisting of 9 uniformly spaced elements, separated by 0.5λ. The reflection coefficients are $\rho_1(\omega) = 1$ and $\rho_2(\omega) = 0.5$. A (low-level) complex-valued white Gaussian noise is added to the simulated frequency response matrix (FRM).

We assume a two-dimensional geometry where the antenna elements are line sources and the targets are line targets all embedded in a homogeneous background and perpendicular to a single plane and all multiple scattering is ignored. From a purely mathematical point-of-view one can just as well consider the antenna elements and the scatterers as simply points in a two-dimensional space. We take this latter view in the following discussion. In the two-dimensional case the appropriate Green function is given by

$$G(\mathbf{R},\mathbf{X}) = -\frac{j}{4} H_0\left(\frac{2\pi}{\lambda}\|\mathbf{R}-\mathbf{X}\|\right)$$

where $H_0(\cdot)$ is the zero order Hankel function of the first kind. It can be shown that in the configuration we consider here the matrix $\mathcal{G}(\omega)$ is guaranteed to have full column rank [7] and, therefore, rank $\mathcal{H}(\omega) =$ rank $\mathcal{G}(\omega) = L = 2$.

Since there are two targets there are two dominant eigenvalues with associated signal space eigenvectors, corresponding to the two well-resolved targets that are separated by two wavelengths. The magnitude of the focused eigen-wavefields, generated from the eigenvectors of the time-reversal matrix, is shown in Fig. 1. We have superimposed an $\mathbf{x}$ at the actual target locations to show that the wavefields tend to peak in the vicinity of the targets.

In this example the targets are well-resolved so that their separate eigen-wavefields do not overlap significantly. However, the same does not hold when the targets are not well resolved, or when the spacing between antenna elements is increased. Moreover, even in this well-resolved example the depth resolution generated by the classical time-reversal images is not very good. Indeed, a close scrutiny of the images in Fig. 1 shows that the maxima do not occur at the exact target locations. Clearly, the depth resolution associated with the time-reversal method is much poorer than is its transversal resolution.

In contrast to the time-reversal eigen-wavefields, the computed MUSIC-type pseudo-spectrum contains only two very sharp peaks, making it possible to obtain very accurate estimates of the scatterers' locations (see Fig. 1). Moreover, the same holds true even when the targets are not well-resolved, or when the spacing between the antenna elements is increased.

6. CONCLUDING REMARKS

We have reviewed the theory of time-reversal imaging using multi-static data and re-interpreted it in the framework of subspace-based signal processing. In particular, we have shown how to employ the *frequency response matrix* (and the derived time-reversal matrix) in place of the array covariance matrix normally used in MUSIC, to generate a *pseudo-spectrum* that yields accurate location estimates of coherent point scatterers from near field multi-static data. The theory was developed for ideal point antennas and point scatterers in arbitrary backgrounds, and ignored all multiple scattering between the scatterers. The simulations treated the case of two-dimensional line antennas and line scatterers in a uniform background. All of the material was developed in the frequency domain and the simulations only treated a single frequency component (the monochromatic case) although generalization to multiple frequencies in both the theory and simulations is straightforward. Future work will concentrate on including the effects of multiple scattering and complex extended objects, and extending our technique to these more general situations.

REFERENCES

[1] C. Prada, L. Thomas and M. Fink, "The Iterative Time Reversal Process: Analysis of the Convergence," *Journal of the Acoustical Society of America*, 97:62-71, 1995.

[2] C. Prada, S. Manneville, D. Spoliansky and M. Fink, "Decomposition of the Time Reversal Operator: Detection and Selective Focusing on Two Scatterers," *Journal of the Acoustical Society of America*, 99:2067-2076, 1996.

[3] R.K. Snieder and J.A. Scales, "Time-Reversed Imaging as a Diagnostic of Wave and Particle Chaos," *Physical Review E*, 58:5668-5675, 1998.

[4] N. Mordant, C. Prada, and M. Fink, "Highly Resolved Detection and Selective Focusing in a Waveguide," *Journal of the Acoustical Society of America*, 105:2634-2642, 1999.

[5] H. Krim and M. Viberg, "Two Decades of Signal Processing: The Parametric Approach," *IEEE Signal Processing Magazine*, 13:67-94, July 1996.

[6] P. Stoica and R. Moses, *Introduction to Spectral Analysis*, Prentice Hall, New Jersey, 1997.

[7] A.J. Devaney, "Super-Resolution Processing of Multistatic Data using Time-reversal and MUSIC," submitted to the *IEEE Transactions on Image Processing*, 1999.

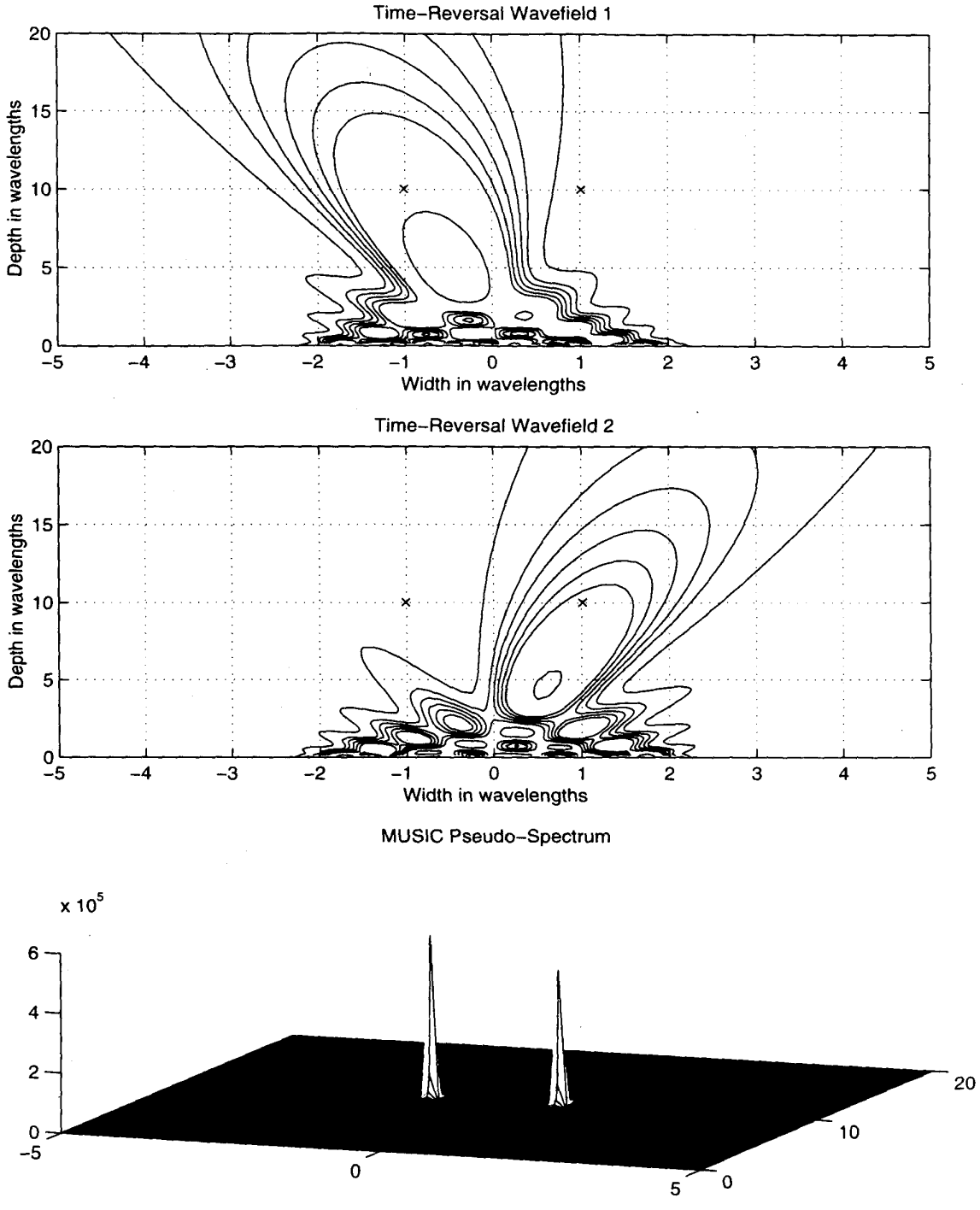

Figure 1: Performance comparison: time-reversal wavefields vs. the MUSIC pseudo-spectrum